A new supported TiO₂ film deposited on stainless steel for the photocatalytic degradation of contaminants of emerging concern

S. Murgolo[1], V. Yargeau[2], R. Gerbasi[3], F. Visentin[3], N. El Habra[3],

G. Ricco[4], I. Lacchetti[5,6], M. Carere[5], M. L. Curri[7], G. Mascolo[1]*

(1) CNR, Water Research Institute, Via F. De Blasio 5, 70132 Bari, Italy.

(2) McGill University, Department of Chemical Engineering, University Street, Montreal, Quebec, Canada.

(3) CNR, Institute of Condensed Matter Chemistry and Energy Technologies, Corso Stati Uniti 4, Padova, Italy.

(4) Regional Environmental Protection Agency, Via Oberdan 16, 70121 Bari, Italy.

(5) National Institute of Health, Department of Environment and Primary Prevent Unit Soil and Waste, Viale Regina Elena 299, Rome, Italy.

(6) CNR, Water Research Institute, Area della Ricerca RM1, Monterotondo (Rome), Italy.

(7) CNR, Institute for Physical and Chemical Processes, Via Orabona 4, 70126 Bari, Italy.

* Corresponding author. Tel.: +39 080 5820519; fax: +39 080 5313365.

e-mail address*:* giuseppe.mascolo@ba.irsa.cnr.it (G. Mascolo).

Abstract

A new supported catalyst composed of a nanostructured TiO_2 film deposited on a stainless steel mesh (nanoTiO$_2$-SS) using the Metal Organic Chemical Vapour Deposition (MOCVD) technique was evaluated for the photocatalytic degradation of a mixture of contaminants of emerging concern. Results showed that under the oxidative conditions tested, the nanoTiO$_2$-SS catalyst had better performance in degrading the target contaminants than direct photolysis and photocatalysis using the conventional TiO_2 Degussa P25 catalyst at the same amount of TiO_2 participating to the photocatalysis. Specifically, the rate of removal of warfarin and trimethoprim obtained with the new catalyst was twice the one observed using TiO_2 Degussa P25 and approximately 1.6 times faster for metoprolol, carbamazepine and gemfibrozil. An evaluation of the electrical energy per order magnitude of removal (EE/O) confirmed the better performance of the new catalyst (24.3-31.8 kWh m^{-3} rather than 32.8-39.3 kWh m^{-3} for conventional TiO_2) and that the performance is compound-dependent. Toxicity testing revealed that some assays are suitable for the investigation of bioactivity of treated waters containing contaminants of emerging concern at μg L^{-1} level. Specifically, the AMES Fluctuation Test, Fish Embryo Acute Toxicity Test and Green alga *Selenastrum capricornutum* test provided valuable results for an environmental impact assessment. On the other hand, the *Daphnia magna* and *Vibrio fischeri* acute toxicity tests were not sensitive enough to detect bioactivity in the samples analysed without prior pre-concentration.

Keywords

TiO_2-based nanostructured catalyst, Contaminants of Emerging Concern, Electrical Energy per Order, Photocatalysis, Toxicity, Transformation Products.

1. Introduction

Research on various wastewater treatment technologies have demonstrated that conventional wastewater treatment plants (WWTPs), mainly based on physicochemical and biological processes, do not efficiently remove a wide variety of organic pollutants [1, 2]. Pharmaceuticals and personal-care products (PPCPs), endocrine disruptor compounds (EDCs), illicit drugs, anticancer drugs, flame retardants, pesticides, perfluorinated compounds and other xenobiotic substances, are known to enter the wastewater network at concentrations in the $\mu g\ L^{-1}$-$ng\ L^{-1}$ range. The main sources of these contaminants in the wastewater and aquatic ecosystems are anthropic activities as well as from landfill leachates, runoff from agriculture, livestock and aquaculture [3]. The presence of these contaminants in the environment has been shown to cause long-term ecological effects such as loss of habitats and biodiversity, feminization of fish, development of microbiological resistance and accumulation in soil, plants and animals [4-6].

Organic pollutants classified as contaminants of emerging concern (CECs) consist of compounds that are not yet regulated and have no discharge limits but have raised concerns and are often on priority lists of various regulatory agencies. The relevance of addressing the issue of organic pollutants was acknowledged by the Directive 2013/39/EU [7, 8] listing priority substances and further supported by the implementation of Decision 2015/495 on March 20, 2015 establishing a watch list including 10 target substances for Union-wide monitoring.

In this context, significant research effort on wastewater treatment aims at finding effective technologies for CECs removal. Advanced oxidation processes (AOPs) based on the action of highly reactive and non-selective oxidants such as hydroxyl radicals (E^0=2.81 V) have been identified as promising technologies for degrading such compounds [9, 10]. Numerous publications have identified AOPs as promising technologies applicable as pre-treatment to biological processes or post-treatment, namely tertiary treatment processes [11-13]. The integration of AOPs prior to biological treatment provides a more biodegradable effluent, which can be further treated using

conventional biological processes that are cheaper that other treatment types and shortens the residence time required in biological treatment steps. Using this integrated approach, the oxidant requirements is less than one required by a configuration placing the AOPs as standalone tertiary treatment. However, the integration of AOPs requires special attention considering that AOPs are known to produce oxidizing agents inhibiting the growth of beneficial microorganisms [14]. In addition, heterogeneous photocatalysis is an attractive AOP due to the absence of addition of chemicals to the treated effluent, making the process environmental friendly compare to other chemical-based treatment [15-18].

Irradiation of TiO_2 with photon having an energy equal or higher than TiO_2 band gap (3.2 eV for anatase, 3.0 eV for rutile and ~3.2 eV for brookite) promotes an electron from the valance band to conduction band (e_{CB}^-), and leaves an electronic vacancy or hole (h_{VB}^+) in the valance band. This hole is highly oxidative and rapidly reacts with surface sorbed organic molecules leading to their degradation. Hydroxyl radicals are also generated through the oxidation of adsorbed water molecules or hydroxyl ions [19, 20], further contributing to the degradation of the contaminants. The bench-mark catalyst, namely TiO_2 Degussa P25, is generally employed as an aqueous suspension although several studies investigated the immobilization of the catalyst onto numerous substrates in order to facilitate recovery and reuse of the catalyst [21-24]. Immobilization of catalysts is required to obtain a scalable an economically viable process for water treatment. However, the efficiency of treatment in heterogeneous reactive systems relies heavily on the adsorption of reactants at the active sites of the catalyst surface while the immobilization of the catalyst inevitably reduces the active surface leading to a loss of photocatalytic activity. Because of the high surface-to-volume ratio leading to a much higher active sites density, TiO_2 nanoparticles (NPs) offer a way to overcome this problem. Another benefit of the nano-size particles is that the photo-generated charges can easily migrate toward the surface of the catalyst leading to a lower probability of bulk recombination [25, 26]. As with micro-sized materials, the immobilization of the

NPs TiO$_2$ prevents their leaching into water, thus strongly limiting the potential risks of dispersion of NPs into the environment.

The mineralization levels achieved using oxidative processes operated at practical operating conditions have been determined as being quite low, leading to a growing interest in the detection and identification of the transformation products resulting from the application of AOPs [27, 28], as well as in the evaluation of the residual toxicity of the treated effluents by monitoring responses in test organisms representative of the receiving waters where the treated effluents are to be discharged [29-31].

To address the issues raised above, this study investigated fundamental and technological aspects of using novel photocatalytic materials for water treatment. A novel supported catalyst based on a nanostructured TiO$_2$ film deposited on a stainless steel mesh (nanoTiO$_2$-SS) by Metal Organic Chemical Vapour Deposition (MOCVD) technique was developed and tested for its performance in term of degradation of a mixture of 10 CECs present at low concentration (μg L^{-1} range). Photolytic and photocatalytic experiments were performed using groundwater as a matrix and employing a pilot scale system equipped with a Hg-UV lamp ($\lambda = 254$ nm). Photolysis and photocatalysis using the conventional TiO$_2$ Degussa P25 catalyst were used as reference treatments (controls). Performance was evaluated based on degradation kinetics of target contaminants and the Electrical Energy per Order (EE/O) parameter, namely the electrical energy amount that is needed for lowering the concentration of a single compound by one order of magnitude (90%) per volume unit (usually 1 m^3) of water treated [32-34]. In addition, the risk of forming transformation products with higher toxicity than their parent compounds was evaluated by monitoring changes in toxicity using several acute toxicity tests covering various trophic levels (*Vibrio fischeri* acute toxicity test, *Daphnia magna* acute toxicity test, Green alga *Selenastrum capricornutum* test, AMES Fluctuation test and Fish Embryo Acute Toxicity Test) and by a preliminary investigation of the transformation products using liquid chromatography coupled to high-resolution mass spectrometry (LC-HRMS).

2. Materials and methods

2.1 Organic pollutants and groundwater characteristics

The mixture of organic pollutants was defined to represent different classes of contaminants of emerging concern. It included warfarin, trimethoprim, metoprolol, carbamazepine, gemfibrozil, terbutaline, iopromide, 2,4 dihydroxy-benzophenone (BP-1), perfluorooctanesulfonic acid (PFOS), perfluorooctanoic acid (PFOA). The selected PPCPs and perfluorinated compounds (Sigma-Aldrich) along with their chemical structures and main characteristics are listed in Table S1 of the Supplementary Material.

Solutions were freshly prepared in filtered (0.45 μm) groundwater by spiking the target compounds to a concentration in the range of 200-400 μg L^{-1}. The groundwater collected from a well at a depth of approximately 30 m was characterized in terms of main water characteristics (pH, conductivity, COD, alkalinity, hardness and concentration of total nitrogen, total phosphorous, NH_4^+, NO_2^-, NO_3^-) using standard methods (Table S2). Solvents and chemicals (methanol and ammonium acetate) employed for both the chemical analyses and standard solutions preparation were HPLC grade (Riedel-de Haën, Baker). A Milli-Q Gradient A-10 (Millipore) system was used to prepare the ultrapure water (18.2 MΩcm, organic carbon ≤ 4μg/L) used for the preparation of eluents for ultra-high pressure liquid chromatography (UPLC) and standard solutions. The conventional catalyst employed for the photocatalytic control experiments was Degussa (Evonik) P25, which consists of anatase and rutile crystallites with a ratio typically of 80:20, a surface area of 50 m^{2}g^{-1} and a average diameter of 30 nm.

2.2 MOCVD nanostructured TiO₂ film synthesis

CVD produces thin solid films from chemical precursors in the vapor phase, which are carried into a heated chamber containing the objects to be coated. Chemical reactions occur typically on heated substrates, resulting in the deposition of a thin film, accompanied by the production of chemical by-products that are exhausted out of the chamber along with unreacted precursor vapors. When the precursor is a metal-organic compound, the technique is indicated as MOCVD and permits the deposition at relatively low temperatures (i.e. 300-400°C). This technique is widely used to prepare thin films with high quality, high uniformity and controlled properties [35, 36]. It offers many benefits such as high deposition rates, inherent flexibility, excellent conformal step coverage and adaptability to large scale processing also on complex substrates.

Titanium tetra-isopropoxide $[Ti(O^iPr)_4]$ (TTIP, 97%, where $-O^iPr$ means $-OCH(CH_3)_2$) from Sigma-Aldrich was used as the precursor (without further purification). MOCVD experiments were carried out in a horizontal hot-wall reactor heated at a mean temperature of 400°C, whose details and main operating parameters are reported elsewhere [37, 38].

TiO₂ films were deposited on stainless steel meshes (35 µm hole size) utilizing a 8x20 cm rectangular mesh substrate for each deposition. The so obtained nanostructured anatase TiO₂ films (with an average thickness of 1500 nm) are referred to in this paper as nanoTiO₂-SS.

Surface morphology was investigated by scanning electron microscopy (SEM) using a Fei Quanta 200 Field Emission Gun-Environmental Scanning Electron Microscopy (FEG-ESEM), in high vacuum mode and with acceleration voltage of about 5 kV. The structural characteristics were studied by X-ray diffraction (XRD) analysis, employing a Philips PW 3710 X-Ray diffractometer in Bragg-Brentano geometry using the Cu Kα radiation (40 kV, 30 mA, λ = 1.54056 Å).

2.3 Experimental setup

A 0.5 L flow reactor equipped with a 40 W Hg low pressure UV lamp (λ=254 nm, fluence rate 50 mW cm^{-2}) was used in recirculation mode to perform the photolysis or photocatalytic experiments. Figure S1 shows the reactor (volume of solution treated 2 L, recirculation flow 6 L h^{-1}) used to perform the photocatalytic degradation experiments using the newly developed nanoTiO$_2$-SS supported catalysts as well as the three control conditions: (i) hydrolysis (with no TiO$_2$ and UV radiation), (ii) photolysis (with UV radiation solely), (iii) photocatalysis (using TiO$_2$ P25). It is worth mentioning that the employed recirculation flow rate did not lead to limitations of external mass transfer on the photocatalytic degradation.

Each test was carried out by placing in the reactor the freshly prepared aqueous solution of organic pollutants and sampling of a first aliquot, corresponding to the time zero sample. For the UV/TiO$_2$ experiments the catalyst was in the range 50-200 mg L^{-1} TiO$_2$ Degussa P25 or three nanoTiO$_2$-SS meshes (8x20 cm each, 35 μm hole size) with an average film thickness of 1500 nm wrapped side by side around the circumference of the quartz probe containing the UV lamp in order to cover almost the entire length of the quartz tube (see dimensions of the reactor in Figure S1. For the latter case it must be noted that not all the TiO$_2$ thickness is active during the photocatalytic tests. Indeed, taking into account the UV absorption length, it is possible to estimate that the effective TiO$_2$ thickness for photocatalysis is lower than 100 nm [39] resulting in an active surface area of about 0.116 mg cm^{-2} (1 cm^2 of mesh corresponds to 2.97 cm^2 of surface covered by TiO$_2$, and the anatase has a density of 3.90 g cm^{-3}). For the three meshes, this corresponds to a total useful TiO$_2$ quantity of 55 mg, which is comparable to the quantity of TiO$_2$ Degussa used at 100 mg L^{-1} (50 mg in the 0.5 L reactor volume). For the UV/TiO$_2$ experiments, the catalyst was first equilibrated in the dark for 30-60 min with the solution to be treated. Another aliquot was collected after equilibration in order to quantify the potential adsorption of the target compounds on the catalyst surface. The lamp was then turned on and sampling was done at regular time intervals over a period of 60 min.

Temperature remained constant over the treatment time and pH did not change significantly, most likely because of the buffer capacity of the groundwater employed (Table S2). At the end of the treatment, the photocatalyst was recovered from the aqueous solution in order to evaluate possible reuse in subsequent treatment cycles. The aqueous samples collected were centrifuged (10000 rpm x 20 min) before being placed in vials for analysis by UPLC-HRMS.

2.4 Toxicity tests

The toxicity tests carried out on samples collected during photolytic and photocatalytic treatments include (i) Daphnia magna Strauss (Cladocera, Crustacea) – acute toxicity tests (UNI EN ISO 6341:2013); (ii) *Vibrio fischeri* – test with luminescent bacteria (UNI EN ISO 11348-3:2009). The inhibition of light emission by cultures of *Vibrio fischeri* (NRRL B-11177) was determined by means of batch test. This was accomplished by combining specific volumes of the test sample or the diluted sample with the luminescent bacteria suspension in a test tube. The test criterion is the luminescence, measured after contact time of 30 min, taking into account of correction factor (f_{kt}), which is a measure of intensity changes of control samples during the exposure time. The amount of light emitted in the sample was used to determine the sample's relative toxicity, which can then be compared to the standard reference's toxicity. As the toxicant's concentration increases, bacterial light emissions decrease in a dose-dependent manner; (iii) Green Alga *Selenastrum capricornutum* (UNI EN ISO 8692:2012). An inoculum of algal strains in exponential phase (bred for several generations in a specific medium) was placed in contact with different concentrations of the sample. The sample was diluted by mixing a suitable amount of medium to the sample itself. The batch of analysis thus prepared (algal inoculum + diluted samples) was incubated for a period of 72 ± 2 h during which the cell density was measured every 24 h. The inhibition was measured as a reduction in the kinetics of algal growth compared to the control sample. Each sample was tested with the alga *Pseudokirchneriella subcapitata*, green algae Sphaeropleales (Chlorophyta, Chlorophyceae), using the above described procedure; (iv) AMES Fluctuation test (mutagenicity test) whose

experimental description is reported elsewhere [40]; (v) Fish Embryo Acute Toxicity (FET) test (OECD 236). The zebrafish embryo toxicity test was based on a 96 h exposure of newly fertilized eggs of *Danio rerio* to the sample. The test was performed in 24-well plates and incubated at 26.0 ± 1.0 °C. As ecotoxicological endpoints, coagulation of eggs and embryos failure to develop somites, lack of heart-beat as well as non-detachment of the tail from the yolk, were observed and recorded daily. At the end of the exposure period, acute toxicity was determined based on a positive outcome (ecotoxicological endpoints) recorded in any of the four apical tests. Dilution water controls were also carried out as required in the method both as negative control and as internal plate controls. In addition, a positive control by a solution of 3,4-dichloroaniline at 4 mg/L was performed. Results are expressed as LC50 or as the sum of daily acute toxicity values obtained and reported in cumulative lethal percentages.

2.5 Chemical analysis

The residual concentration of the investigated compounds at various reaction times as well as the investigation of transformation products were carried out using an Ultimate 3000 System (Thermo Fisher Scientific) equipped with an autosampler, temperature-controlled column compartment and UV detector as a chromatographic system that was interfaced with a high-resolution mass spectrometer, TripleTOF® 5600+ System (AB Sciex) equipped with a duo-spray ion source that was operated in electrospray (ESI) mode in positive and negative ion modes. MS analysis was carried out by an information dependent analysis (IDA) method that includes a survey scan in TOF-MS and, after background subtraction, the isolation and fragmentation in the collision cell of the four most intense ions using parameters listed in Table S3.

The chromatography was performed using 5 μL samples injected and eluted at 0.200 mL min^{-1} through a BEH C18 column, 2.1 x 150 mm, 1.7 μm, with a binary gradient consisting of 1.5 mM ammonium in water (A) and 1.5 mM ammonium in methanol (B). The gradient started from 5 % B

then was linearly increased to 95 % in 10 min and held for 7 min. At the end of each run the system was equilibrated for 5 min. Data processing was performed by MetabolitePilot 1.5, PeakView 2.2, MasterView 1.1 and MultiQuan 3.0.2 (AB Sciex).

3. Results and discussion

3.1 NanoTiO$_2$-SS synthesis and characterization

Stainless steel meshes (holes of 35 μm diameter) were used as the substrate, utilizing a 8x20 cm rectangular mesh sample for each deposition. During the MOCVD process the deposition time is proportional to the thickness of the deposited film; a deposition time of 4500 s was chosen with the aim of obtaining a corresponding TiO$_2$ film thickness of about 1500 nm and the appropriate surficial characteristics in terms of crystallite size and roughness [37].

XRD analysis of the stainless steel meshes coated by TiO$_2$ indicated the formation of TiO$_2$ in the polycrystalline anatase phase (ICDD 00-021-1272) with crystallite dimension of about 30 nm calculated by the Scherrer formula (Figure S2). The surficial morphology of the film reported in Figure S3 (A) shows a typical facetted texture, while the thickness was evidenced in Figure S3 (B) with a mean value of about 1500 nm.

Moreover, it should be underlined that the CVD processes permit to uniformly cover the meshes including the inside of the hole walls, resulting in a greater effective photocatalytic area. This type of supported photocatalyst is firmly immobilized on the substrate and will not be dispersed in the testing solutions.

3.2 Direct photolysis of investigated contaminants

The photocatalytic degradation of pollutants in water matrices involves two types of reaction happening in parallel: photolysis and photocatalysis. In order to estimate the contribution of the new

nanoTiO$_2$-SS catalyst in removing the target pollutants, reference experiments were conducted in presence of the light source only (photolysis experiments – absorption of radiation i.e. energy, which leads to a break-up of the compounds). For each treatment tested, the reaction rate constant k (min^{-1}) was determined for each single pollutant present in aqueous matrix. The obtained values were used to determine the performance of the treatment in degrading the target pollutants and provided a comparison point for the efficiency of the newly synthesized nanoTiO$_2$-SS relative to the conventional TiO$_2$ Degussa P25 catalysts and to the photolytic treatment performed under same experimental conditions. Results reported in Figure 1a (three replicates photolytic experiments i.e. Exp1, Exp2, Exp3) showed that during photolysis performed in the 0.5 L flow reactor (Hg-UV lamp), the most recalcitrant pollutants were warfarin, trimethoprim, carbamazepine, metoprolol, and gemfibrozil with first-order kinetics constant values in the range 0.03 min^{-1}- 0.05 min^{-1}.

Conversely, iopromide, terbutaline and 2,4-dihydroxybenzophenone were quickly removed by photolysis, within 5-10 minutes of treatment (Figure 1b), and the kinetics constant could not be determined. Under the treatment conditions tested, no photolytic degradation was observed for PFOA and PFOS as shown in Figure 1b. The organic pollutants that were in a range of measurable kinetics of removal (warfarin, trimethoprim, carbamazepine, metoprolol, and gemfibrozil) were selected to determine the potential of the new nanoTiO$_2$-SS catalyst at improving the removal of CECs during photocatalytic treatment. Possible improvement for the removal of PFOS and PFOA by photocatalysis was also investigated.

3.3   Photocatalytic removal of CECs

The degradation kinetics of the investigated mixture of CECs in groundwater followed the model of Langmuir-Hinshelwood showing first-order kinetics for all the investigated contaminants (data not shown). Figure 2 shows the first-order kinetic constants obtained during photocatalytic treatments of CECs employing nanoTiO$_2$-SS, conventional suspended catalysts TiO$_2$ Degussa P25 (in the

range 50-200 mg L^{-1}) and photolytic treatment. No measurable removals were observed, under all conditions, for PFOS and PFOA. Control experiments performed in the dark (data not shown) and in the presence of catalysts indicated that the amount of CECs adsorbed on the catalyst was negligible. The lack of changes in concentration during exposure to catalyst also indicated that hydrolysis of the target pollutants due to the catalysts did not occur.

According to the results shown in Figure 2, degradation rate by TiO$_2$ Degussa P25 increased at higher TiO$_2$ concentration in the range 50-200 mg L^{-1}. However, for a comparison with the nanoTiO$_2$-SS, the same amount of TiO$_2$ participating to the reaction should be considered in the two cases. As mentioned in section 2.3, for the nanoTiO$_2$-SS the effective TiO$_2$ thickness participating to photocatalysis is lower than 100 nm resulting in an active surface area of about 0.116 mg cm^{-2} and then to a total useful TiO$_2$ quantity of 55 mg. It follows that the comparison should be performed with the suspended TiO$_2$ Degussa used at 100 mg L^{-1} corresponding to 50 mg TiO$_2$ present in the 0.5 L reactor volume. The nanoTiO$_2$-SS demonstrated a better performance in degrading the target pollutants in groundwater when compared to photolysis and photocatalysis using conventional TiO$_2$. The performance of the new catalyst significantly surpassed the TiO$_2$ Degussa P25 despite the fact that the active surface of immobilized catalyst is reduced upon deposition onto a surface. The ratio between the calculated kinetic constants $k_{nanoTiO2\text{-}SS}/k_{TiO2\ DegP25}$ indicated that the rate of removal with the new catalyst was approximately 1.2-1.4 times faster the one observed using TiO$_2$ Degussa P25 (100 mg L^{-1}). In addition, Figure 2 also shows that the CECs degradation rates with the nanoTiO$_2$-SS were comparable to those obtained with TiO$_2$ Degussa P25 at 200 mg L^{-1}, namely when using twofold amount of TiO$_2$ as a suspension. At the end of the photocatalytic treatment using the nanoTiO$_2$-SS, the catalyst was recovered and reused for multiple reaction cycles. Indeed after ten cycles the performance of the catalyst was found in the range of 75-90%, as a function of the organic pollutant composition

3.4   Energy requirement for the removal of CECs

From the degradation profiles of each investigated organic contaminants as a function of the UV dose applied, the Electrical Energy per Order or EE/O parameter (kWh/m³) was calculated using the following equation [32-34]:

$$UVdose(kWh/m^3) = EE/O \; x \log(Ci/Cf)$$

where C_i and C_f are the initial and final pollutant concentrations, respectively. The UV dose parameter combines flow rate, residence time and light intensity into a single term given by the following expression:

$$UVdose(kWh/m^3) = \frac{1000 \; x \; UV \; power \; (kW) \; x \; t \; (min)}{60 \; x \; V \; (L)}$$

where V is the volume (L) of the treated water. From these two equations, and knowing the kinetic expression of the reaction rate $ln \; (C_i/C_f) = k \; t$, EE/O can be defined or calculated as follows:

$$EE/O(kWh/m^3) = \frac{38.4 \; x \; UV \; power \; (kW)}{V \; (L) \; x \; k \; (min^{-1})}$$

where k is the first-order rate constant (min^{-1}) for the disappearance or degradation of the target pollutant concentration. Comparing the EE/O values obtained for photolysis and photocatalysis reactions (Table 1) indicated that photocatalysis treatment employing the nanoTiO$_2$-SS slightly lowered the energy requirement for a given removal for all the emerging organic pollutants tested (24.3-31.8 kWh m^{-3} rather than 32.8-39.3 kWh m^{-3} for conventional TiO$_2$ at 100 mg L^{-1}).

These results confirm the slightly better performance offered by the nanoTiO$_2$-SS using another evaluation criteria, the electrical energy per order of degradation commonly used in the water treatment industry to compare different UV-based technologies. These further indicate that the performance in degrading target pollutants is compound-dependent. For trimethoprim, the compound with the biggest difference between photoloysis and nanoTiO$_2$-SS photocatalysis, it is possible to conclude that photocatalysis had an EE/O value (28.7 kWh m^{-3}) almost five times lower that for photoloysis (129 kWh m^{-3}).

3.5 Evaluation of toxicity of the treated water

To further evaluate the efficiency of treatment, toxicity tests were performed on samples collected during treatment using nanoTiO$_2$-SS and control conditions (photolysis and photocatalysis using Degussa P25) at set reaction times of 0 min, 7.5 min and 60 min. All treatments were performed in duplicates and the results of toxicity tests represent an average of the values obtained performing the specific toxicity test on both replicates for each investigated reaction time and treatment type.

Table 2 summarizes the results obtained from the acute toxicity tests performed with *Daphnia magna Strauss, Vibrio fischeri* and *Green Alga Selenastrum Capricornutum* as well as the AMES Fluctation test. For the inhibition of the mobility of *Daphnia Magna Straus* (UNI EN ISO 6341:2013), expressed as % of mobility inhibition, results (data not shown) indicated no toxicity (<10% of mobility inhibition) in the initial solution and no increase in toxicity during treatment for all the conditions tested. The effects might have been lower than the limit of detection of the assays. The *Vibrio fischeri* results (UNI EN ISO 11448-3:2009) (Table 2) are expressed as percentages of bioluminescence inhibition for the test bacteria. Based on UNI EN ISO 11348-3 samples showing a bioluminescence inhibition of less than 20% are considered non-toxic. The percentage of inhibition of bioluminescence was less than 20% in the samples collected at time 0 and in all samples treated for 60 min. However, some transient increase in the toxicity, to level barely above the limit of non-

toxic effect, 23.7% and 21.5% (reaction time = 7.5 min), were observed for samples collected during photocatalytic treatments in presence of the nanoTiO$_2$-SS and the conventional TiO$_2$ Degussa P25, respectively.

The results obtained using the more sensitive toxicity test, i.e. Green Alga *Selenastrum capricornutum* test (UNI EN ISO 8692:2012), revealed a decrease in toxicity after 60 minutes of reaction for all the investigated treatments. As for AMES Fluctation test the results summarized in Table 2 are expressed as a mutagenicity ratio (MR= number of positive wells in samples/number of positive wells in the negative control). Statistical significance that occurred in the number of positive wells compared with spontaneous revertant wells was determined using the chi-square (χ^2) analysis [41]. According to the results in Table 2, all the samples demonstrated a mutagenic effect. While a decrease in toxicity was observed after 60 min of reaction for the photocatalytic treatment in presence of the supported TiO$_2$ on stainless steel (MR=2.5), increase mutagenicity was observed for the same treatment after 7.5 min.

Finally, daily lethal percentages of *Danio rerio* embryos for the two replicates up to 96 h (4 d) are listed in Table 2. The untreated sample had an initial toxicity for fish embryos (reaction time 0 min), with a value of 50 % mortality. Mortality percentages for each performed treatment were compared with the initial value obtained at time 0 min. Toxicity levels remain fairly constant for all reaction time with a maximum increment of 15 % at 7.5 min for photocatalytic treatment with nanoTiO$_2$-SS. The OECD Guideline recommends also to note and report any secondary effects of embryo abnormalities at the end of the tests, with particular attention to the hatching of eggs. The eggs exposed to samples collected during photolysis and conventional Degussa P25 catalyst treatment showed a significant delay in hatching at the time points 7.5 min and 60 min. Only the treatment with nanoTiO$_2$-SS allows the normal development of embryos and the hatching of eggs without any delays in hatching.

Overall, toxicity results evidenced that the AMES Fluctuation Test and Fish Embryo Acute Toxicity (FET) test gave similar results for the treated groundwater samples, namely a slight increase at 7.5 min and then a decrease at 60 min, while test Growth Inhibition test (Green Alga) showed a continuous decrease in toxicity during all the investigated treatment times. Instead, *Daphnia Magna Straus* and *Vibrio fischeri* tests were not sensitive enough to the investigated samples and further sample preparation would be required for these assays.

3.6   Identification of degradation products

Identification of degradation products was mainly performed to verify whether the photocatalytic process carried out with the nanoTiO$_2$-SS catalyst led to different degradation products when compare to the reaction performed with the conventional Degussa P25 catalyst. Accordingly, identification of degradation products was only focused to the most abundant compounds present in the reaction mixtures. Indeed, the complete identification of degradation products formed is a very difficult tasks mainly due to the fact that the reactions were performed with a real water matrix (groundwater) and with a mixture of ten CECs. The main degradation products that were identified are listed in Table 3. For each of them the assignment of elemental composition was made possible by combining high-resolution mass spectrometry data with the information contained in high-resolution mass spectra about the isotopic distribution of ions, defined as spectral accuracy [42]. In addition, for 9 out of 12 compounds, on the basis of the information obtained in single and in tandem high resolution MS mode, it was also possible to propose a chemical structure derived from one of the parent compounds included in the mixture. It is worth noting that the obtained identification can be classified as level 3 (tentative candidates) according to the scheme of identification confidence levels proposed by Schymanski et al. [43]. Results listed in Table 3 show that the main degradation products were derived from five out of the eight pollutants for which degradation was observed, namely terbutaline, warfarin, trimethoprim, BP-1, metoprolol. The

degradation products were mainly formed due to oxidation reaction, namely inserting a hydroxyl group on the aromatic ring, as well as to further reaction leading to a breakdown of the structure of parent compounds. No degradation products of carbamazepine, gemfibrozil and iopromide were identified. This could be inferred to the higher reactivity of these compounds leading to breakdown products that were more polar and thus not amenable to be analyzed by UPLC method employed. The detected degradation products also showed to follow different formation/degradation profiles (Figure S4). Some of them follow a typical bell-shape trend while others were constantly formed during the investigated reaction time. The disappearence of the detected compounds at higher reaction times suggests the further formation of polar degradation products, namely low molecular weight organic acids, as already found in other oxidative processes [44], which are not detectable by conventional reverse phase liquid chromatography.

Table 3 also show that the identified degradation products were not detected for all oxidative treatments tested. Minor differences were found between photocatalysis performed with nanoTiO$_2$-SS and Degussa P25 catalysts suggesting also minor differences in the reaction mechanism. However, further investigation must be performed to demonstrate such a finding.

4. Conclusions

The new supported catalyst nanoTiO$_2$-SS based on nanostructured TiO$_2$ films deposited on a stainless steel mesh for the photocatalytic degradation of a mixture of contaminants of emerging concern in real groundwater proved to offer better performances than the conventional Degussa P25 catalyst. The evaluation of the electrical energy per order magnitude of removal (EE/O) confirmed the better performance of the new catalyst with respect to Degussa P25 and that the performance in degrading the target pollutants is compound-dependent.

The toxicity tests revealed that some of these assays are suitable for the investigation of environmental effects of treated waters containing contaminants of emerging concern at µg L^{-1} level without any particular sample preparation. Specifically, AMES Fluctuation Test, Fish Embryo Acute Toxicity and Growth Inhibition test by Green Alga were able to provide valuable results for an environmental assessment. The toxicity detected by AMES test and FET test in the photolytic treatment and photocatalytic conventional TiO_2 Degussa P25 indicated no decrease of toxicity during these reference reatments, while the algae test reported a decrease of the toxicity. For the new catalyst, a reduction of toxicity was observed based on all the toxicity tests performed except for the FET for which the toxicity remains unchanged. The different trends observed in the suite of ecotoxicological tests can be due to the different mode of action of the chemical substances present in the mixture or the possible synergic specific effects (e.g. mutagenic and embryotoxic) of the mixture. In order to investigate which pollutant of the mixture is the major responsible of the toxicity detected after the treatment it could be useful to apply new methodologies such as for example Effect Direct Analysis (EDA) [45]. Overall, the results underline that the integration of both chemical and toxicological analysis provides a powerful tool for determining the potential hazards associated with contaminants of emerging concern.

Acknowledgement

References

[1] N. Ratola, A. Cincinelli, A. Alves, A. Katsoyiannis, Occurrence of organic microcontaminants in the wastewater treatment process. A mini review, J. Hazard. Mater., 239–240 (2012) 1-18.

[2] Y. Luo, W. Guo, H.H. Ngo, L.D. Nghiem, F.I. Hai, J. Zhang, S. Liang, X.C. Wang, A review on the occurrence of micropollutants in the aquatic environment and their fate and removal during wastewater treatment, Sci. Total Environ., 473–474 (2014) 619-641.

[3] A. Jurado, E. Vàzquez-Suñé, J. Carrera, M. López de Alda, E. Pujades, D. Barceló, Emerging organic contaminants in groundwater in Spain: A review of sources, recent occurrence and fate in a European context, Sci. Total Environ., 440 (2012) 82-94.

[4] M. DeLorenzo, J. Fleming, Individual and Mixture Effects of Selected Pharmaceuticals and Personal Care Products on the Marine Phytoplankton Species Dunaliella tertiolecta, Arch. Environ. Contam. Toxicol., 54 (2008) 203-210.

[5] J.E. Drewes, S. Khan, Water Reuse for Drinking Water Augmentation, in: J. Edzwald (Ed.) Water Quality and Treatment, 6th Edition, American Water Works Association, Denver, Colorado., 2011, pp. 48.

[6] E.K. Muirhead, A.D. Skillman, S.E. Hook, I.R. Schultz, Oral Exposure of PBDE-47 in Fish: Toxicokinetics and Reproductive Effects in Japanese Medaka (Oryzias latipes) and Fathead Minnows (Pimephales promelas), Environ. Sci. Technol., 40 (2005) 523-528.

[7] P. Schröder, B. Helmreich, B. Škrbić, M. Carballa, M. Papa, C. Pastore, Z. Emre, A. Oehmen, A. Langenhoff, M. Molinos, J. Dvarioniene, C. Huber, K.P. Tsagarakis, E. Martinez-Lopez, S.M. Pagano, C. Vogelsang, G. Mascolo, Status of hormones and painkillers in wastewater effluents across several European states—considerations for the EU watch list concerning estradiols and diclofenac, Environ Sci Pollut Res, (2016) 1-32.

[8] A.R. Ribeiro, O.C. Nunes, M.F.R. Pereira, A.M.T. Silva, An overview on the advanced oxidation processes applied for the treatment of water pollutants defined in the recently launched Directive 2013/39/EU, Environ. Int., 75 (2015) 33-51.

[9] M. Klavarioti, D. Mantzavinos, D. Kassinos, Removal of residual pharmaceuticals from aqueous systems by advanced oxidation processes, Environ. Int., 35 (2009) 402-417.

[10] I. Munoz, S. Malato, A. Rodriguez, X. Domnech, Integration of Environmental and Economic Performance of Processes. Case Study on Advanced Oxidation Processes for Wastewater Treatment, J. Adv. Oxid. Technol., 11 (2008) 270-275.

[11] J.L. de Morais, P.P. Zamora, Use of advanced oxidation processes to improve the biodegradability of mature landfill leachates, J. Hazard. Mater., 123 (2005) 181-186.

[12] I. Oller, S. Malato, J.A. Sánchez-Pérez, Combination of Advanced Oxidation Processes and biological treatments for wastewater decontamination--A review, Sci. Total Environ., In Press, doi: 10.1016/j.scitotenv.2010.08.061 (2011).

[13] A. Bernabeu, R.F. Vercher, L. Santos-Juanes, P.J. Simón, C. Lardín, M.A. Martínez, J.A. Vicente, R. González, C. Llosá, A. Arques, A.M. Amat, Solar photocatalysis as a tertiary treatment to remove emerging pollutants from wastewater treatment plant effluents, Catal. Today, 161 (2011) 235-240.

[14] C. Di Iaconi, G. Del Moro, M. De Sanctis, S. Rossetti, A chemically enhanced biological process for lowering operative costs and solid residues of industrial recalcitrant wastewater treatment, Water Res., 44 (2010) 3635-3644.

[15] M.A. Sousa, C. Gonçalves, V.J.P. Vilar, R.A.R. Boaventura, M.F. Alpendurada, Suspended TiO2-assisted photocatalytic degradation of emerging contaminants in a municipal WWTP effluent using a solar pilot plant with CPCs, Chem. Eng. J., 198–199 (2012) 301-309.

[16] M.N. Sugihara, D. Moeller, T. Paul, T.J. Strathmann, TiO2-photocatalyzed transformation of the recalcitrant X-ray contrast agent diatrizoate, Appl. Catal. B-Environ., 129 (2013) 114-122.

[17] L. Prieto-Rodriguez, S. Miralles-Cuevas, I. Oller, A. Agüera, G.L. Puma, S. Malato, Treatment of emerging contaminants in wastewater treatment plants (WWTP) effluents by solar photocatalysis using low TiO2 concentrations, J. Hazard. Mater., 211–212 (2012) 131-137.

[18] P. Raja, A. Bozzi, W.F. Jardim, G. Mascolo, R. Renganathan, J. Kiwi, Reductive/oxidative treatment with superior performance relative to oxidative treatment during the degradation of 4-chlorophenol, Appl. Catal. B-Environ., 59 (2005) 249-257.

[19] M. Pelaez, N.T. Nolan, S.C. Pillai, M.K. Seery, P. Falaras, A.G. Kontos, P.S.M. Dunlop, J.W.J. Hamilton, J.A. Byrne, K. O'Shea, M.H. Entezari, D.D. Dionysiou, A review on the visible light active titanium dioxide photocatalysts for environmental applications, Appl. Catal. B-Environ., 125 (2012) 331-349.

[20] J.A. Dumesic, G.W. Huber, M. Boudart, Principles of Heterogeneous Catalysis, in: Handbook of Heterogeneous Catalysis, Wiley-VCH Verlag GmbH & Co. KGaA, 2008.

[21] R. Comparelli, E. Fanizza, M.L. Curri, P.D. Cozzoli, G. Mascolo, A. Agostiano, UV-induced photocatalytic degradation of azo dyes by organic-capped ZnO nanocrystals immobilized onto substrates, Appl. Catal. B-Environ., 60 (2005) 1-11.

[22] N. Miranda-García, S. Suárez, B. Sánchez, J.M. Coronado, S. Malato, M.I. Maldonado, Photocatalytic degradation of emerging contaminants in municipal wastewater treatment plant effluents using immobilized TiO2 in a solar pilot plant, Appl. Catal. B-Environ., 103 (2011) 294-301.

[23] G. Mascolo, R. Comparelli, M.L. Curri, G. Lovecchio, A. Lopez, A. Agostiano, Photocatalytic degradation of methyl red by TiO2: Comparison of the efficiency of immobilized nanoparticles versus conventional suspended catalyst, J. Hazard. Mater., 142 (2007) 130-137.

[24] A. Panniello, M.L. Curri, D. Diso, A. Licciulli, V. Locaputo, A. Agostiano, R. Comparelli, G. Mascolo, Nanocrystalline TiO 2 based films onto fibers for photocatalytic degradation of organic dye in aqueous solution, Appl. Catal. B-Environ., 121-122 (2012) 190-197.

[25] R. Leary, A. Westwood, Carbonaceous nanomaterials for the enhancement of TiO2 photocatalysis, Carbon, 49 (2011) 741-772.

[26] S. Murgolo, F. Petronella, R. Ciannarella, R. Comparelli, A. Agostiano, M.L. Curri, G. Mascolo, UV and solar-based photocatalytic degradation of organic pollutants by nano-sized TiO2 grown on carbon nanotubes, Catal. Today, 240, Part A (2015) 114-124.

[27] A. Agüera, M.J. Martínez Bueno, A.R. Fernández-Alba, New trends in the analytical determination of emerging contaminants and their transformation products in environmental waters, Environ Sci Pollut Res, 20 (2013) 3496-3515.

[28] D. Fatta-Kassinos, M.I. Vasquez, K. Kümmerer, Transformation products of pharmaceuticals in surface waters and wastewater formed during photolysis and advanced oxidation processes – Degradation, elucidation of byproducts and assessment of their biological potency, Chemosphere, 85 (2011) 693-709.

[29] D. Nasuhoglu, V. Yargeau, D. Berk, Photo-removal of sulfamethoxazole (SMX) by photolytic and photocatalytic processes in a batch reactor under UV-C radiation, J. Hazard. Mater., 186 (2011) 67-75.

[30] J.C.C. da Silva, J.A.R. Teodoro, R.J.d.C.F. Afonso, S.F. Aquino, R. Augusti, Photolysis and photocatalysis of ibuprofen in aqueous medium: characterization of by-products via liquid chromatography coupled to high-resolution mass spectrometry and assessment of their toxicities against Artemia Salina, J. Mass Spectrom., 49 (2014) 145-153.

[31] R. Andreozzi, R. Marotta, G. Pinto, A. Pollio, Carbamazepine in water: persistence in the environment, ozonation treatment and preliminary assessment on algal toxicity, Water Res., 36 (2002) 2869-2877.

[32] G. Mascolo, R. Ciannarella, L. Balest, A. Lopez, Effectiveness of UV-based advanced oxidation processes for the remediation of hydrocarbon pollution in the groundwater: A laboratory investigation, J. Hazard. Mater., 152 (2008) 1138-1145.

[33] N. Daneshvar, A. Aleboyeh, A.R. Khataee, The evaluation of electrical energy per order (EEo) for photooxidative decolorization of four textile dye solutions by the kinetic model, Chemosphere, 59 (2005) 761-767.

[34] AOT Handbook, Calgon Carbon Corporation. Markham, Ontario; Tucson, Arizona, Pittsburgh, PA, 1996.

[35] A. Devi, 'Old Chemistries' for new applications: Perspectives for development of precursors for MOCVD and ALD applications, Coord. Chem. Rev., 257 (2013) 3332-3384.

[36] C.A. Jones, L.M. Hitchman, Chemical Vapour Deposition : Precursors, Processes and Applications, Royal Society of Chemistry, 2008.

[37] R. Gerbasi, M. Bolzan, N. El Habra, G. Rossetto, L. Schiavi, A. Strini, S. Barison, Photocatalytic Activity Dependence on the Structural Orientation of MOCVD TiO2 Anatase Films, J. Electrochem. Soc., 156 (2009) K233-K237.

[38] S. Battiston, M. Minella, R. Gerbasi, F. Visentin, P. Guerriero, A. Leto, G. Pezzotti, E. Miorin, M. Fabrizio, C. Pagura, Growth of titanium dioxide nanopetals induced by single wall carbon nanohorns, Carbon, 48 (2010) 2470-2477.

[39] Z. Zhang, J.T. Yates, Direct Observation of Surface-Mediated Electron−Hole Pair Recombination in TiO2(110), The Journal of Physical Chemistry C, 114 (2010) 3098-3101.

[40] E. Ubomba-Jaswa, P. Fernandez-Ibanez, K.G. McGuigan, A preliminary Ames fluctuation assay assessment of the genotoxicity of drinking water that has been solar disinfected in polyethylene terephthalate (PET) bottles, J Water Health, 8 (2010) 712-719.

[41] R.I. Gilbert, The analysis of fluctuation tests, Mutation Research/Environmental Mutagenesis and Related Subjects, 74 (1980) 283-289.

[42] A. Amorisco, V. Locaputo, C. Pastore, G. Mascolo, Identification of low molecular weight organic acids by ion chromatography/hybrid quadrupole time-of-flight mass spectrometry during Uniblu-A ozonation, Rapid Commun. Mass Spectrom., 27 (2013) 187-199.

[43] E.L. Schymanski, J. Jeon, R. Gulde, K. Fenner, M. Ruff, H.P. Singer, J. Hollender, Identifying Small Molecules via High Resolution Mass Spectrometry: Communicating Confidence, Environ. Sci. Technol., 48 (2014) 2097-2098.

[44] G. Mascolo, A. Lopez, A. Detomaso, G. Lovecchio, Ion chromatography–electrospray mass spectrometry for the identification of low-molecular-weight organic acids during the 2,4-dichlorophenol degradation, J. Chromatogr., 1067 (2005) 191-196.

[45] A.-S. Wernersson, M. Carere, C. Maggi, P. Tusil, P. Soldan, A. James, W. Sanchez, V. Dulio, K. Broeg, G. Reifferscheid, S. Buchinger, H. Maas, E. Van Der Grinten, S. O'Toole, A. Ausili, L. Manfra, L. Marziali, S. Polesello, I. Lacchetti, L. Mancini, K. Lilja, M. Linderoth, T. Lundeberg, B. Fjällborg, T. Porsbring, D.J. Larsson, J. Bengtsson-Palme, L. Förlin, C. Kienle, P. Kunz, E. Vermeirssen, I. Werner, C.D. Robinson, B. Lyons, I. Katsiadaki, C. Whalley, K. den Haan, M. Messiaen, H. Clayton, T. Lettieri, R.N. Carvalho, B.M. Gawlik, H. Hollert, C. Di Paolo, W. Brack, U. Kammann, R. Kase, The European technical report on aquatic effect-based monitoring tools under the water framework directive, Environmental Sciences Europe, 27 (2015) 1-11.

Figure Captions

Figure 1. (a). First order kinetic constants (k) of UV photolytic treatments for removal of investigated organic pollutants in groundwater employing the flow UV. Three replicates used: Exp 1, Exp 2 and Exp 3. (b). Photolytic degradation of iopromide, terbutaline, BP-1, PFOA and PFOS in groundwater employing the flow UV reactor (light source 40 W Hg lamp, reactor volume: 0.5 L, treated volume: 2 L, recirculation flow rate: 6 L h^{-1}).

Figure 2. Photocatalytic performance of TiO_2 supported catalyst on stainless steel as compared to photolysis and conventional Degussa P25 for the removal of target emerging pollutants in groundwater (light source 40W Hg lamp, reactor volume: 0.5 L, treated volume: 2 L, recirculation flow rate: 6 L h^{-1}). Error bars = 1 standard deviation of three replicates.

Table 1. EE/O values obtained for the degradation of CECs in groundwater employing the flow UV reactor operated for photolysis and photocatalysis.

	Electrical Energy per Order of degradation (EE/O) [kWh m^{-3}]				
	Photolysis	Photocatalysis, TiO$_2$ Degussa P25			Photocatalysis, nanoTiO$_2$-SS
		50 mg/L	100 mg/L	200 mg/L	
Trimethoprim	129	59.5	39.1	25.8	28.7
Metoprolol	60.5	39.4	32.8	24.4	24.3
Carbamazepine	116	52.2	39.3	27.1	31.8
Gemfibrozil	78.1	47.8	36.1	25.6	28.4
Warfarin	101	49.6	35	22.8	25.1

Table 2. Acute toxicity tests performed with *Daphnia magna Strauss*, *Vibrio fischeri*, Green Alga *Selenastrum Capricornutum*, AMES Fluctation test and embryo of fish *Danio rerio* (FET).

	Daphnia magna Strauss (% Mobility inhibition)	*Vibrio fischeri* (% Bioluminescence inibition)	*Selenastrum capricornutum* (% Growth Inibition)	*AMES Fluctation test* (Mutagenicity Ratio, MR)	*FET* (% Mortality)
Reaction time = 0 min	< 10	< 20	53.2	3.9	50
Photocatalysis, nanoTiO$_2$-SS					
Reaction time = 7.5 min	< 10	23.7	45.9	5.3	65
Reaction time = 60 min	< 10	< 20	25.7	2.5	63
Photolysis					
Reaction time = 7.5 min	< 10	< 20	48.3	4.4	53
Reaction time = 60 min	< 10	< 20	27.2	4.7	60
Photocatalysis, conventional TiO$_2$ Degussa P25					
Reaction time = 7.5 min	< 10	21.5	49.8	5.2	55
Reaction time = 60 min	< 10	< 20	23.4	6.4	58

Table 3. Degradation products identified during the degradation of a mixture of contaminants of emerging concern in real groundwater by photolysis and photocatalysis using both Degussa P25 and a stainless steel mesh (nanoTiO₂-SS) catalyst.
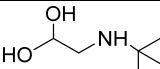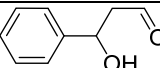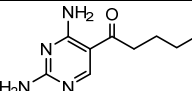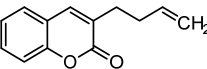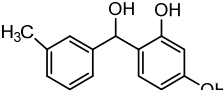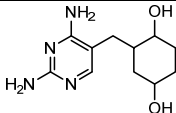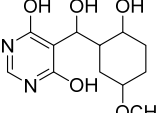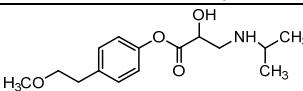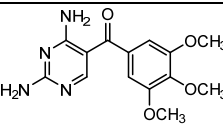
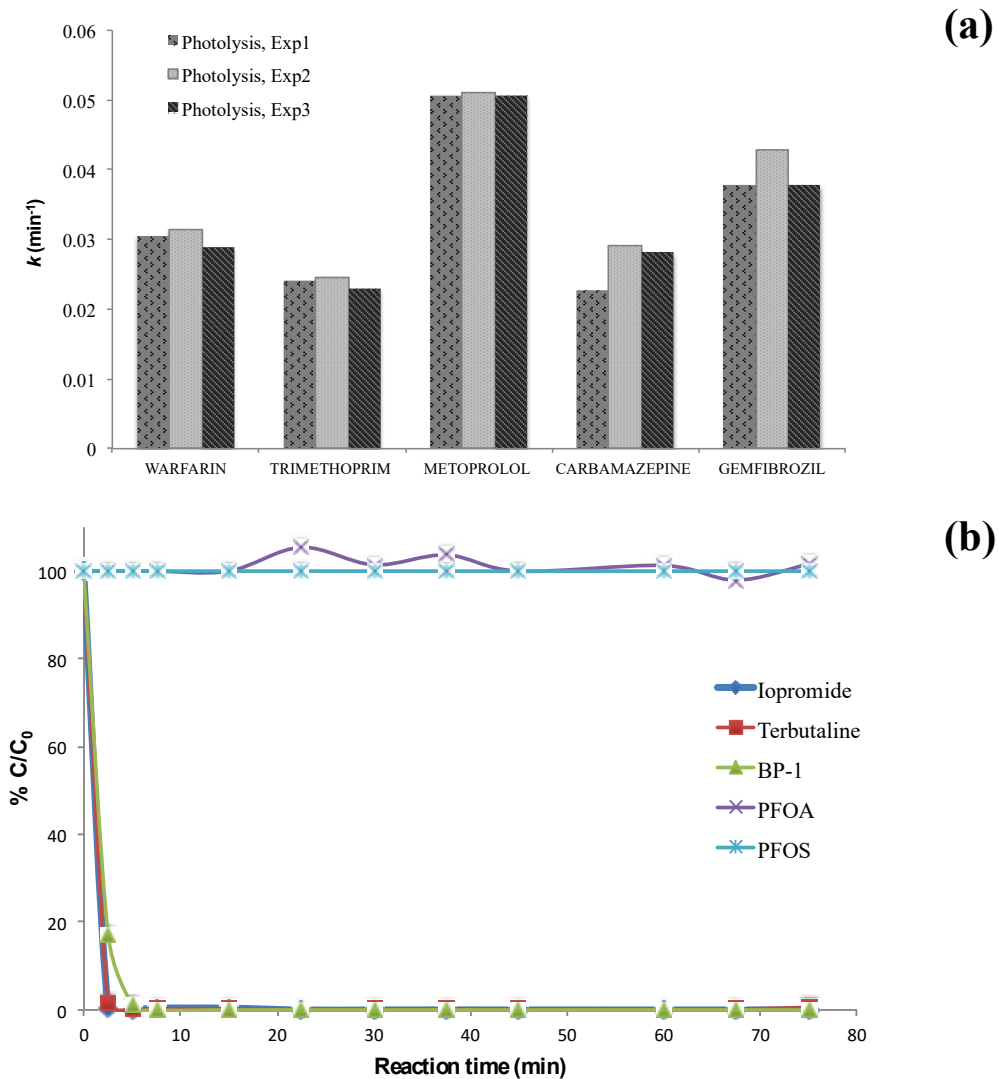|	Measured mass, $[M+H]^+$ (m/z)	Calculated mass (m/z), $[M+H]^+$ (m/z)	Formula	RT (min)	Proposed structure	Parent compound	Identified during reaction with		
							UV	UV/ P25	UV/ nanoTiO₂-SS
TP1	134.1173	134.1176	$C_6H_{15}NO_2$	2.5		Terbutaline	X	X	X
TP2	151.0958	151.0754	$C_9H_{10}O_2$	4.2		Warfarin			X
TP3	195.1240	195.1240	$C_9H_{14}N_4O$	4.9		Trimethoprim			X
TP4	201.0904	201.0910	$C_{13}H_{12}O_2$	11.4		Warfarin	X	X	X
TP5	231.1016	231.1016	$C_{14}H_{14}O_3$	9.1		BP-1		X	X
TP6	239.1503	239.1502	$C_{11}H_{18}N_4O_2$	5.5		Trimethoprim		X	X
TP7	271.1288	271.1289	$C_{12}H_{18}N_2O_5$	6.2		Trimethoprim		X	X
TP8	282.1700	282.1699	$C_{15}H_{23}NO_4$	8		Metoprolol	X	X	X
TP9	295.1387	295.1387	$C_{12}H_{22}O_8$	6.3			X	X	X
TP10	305.1233	305.1244	$C_{14}H_{16}N_4O_4$	8.5		Trimethoprim	X	X	X
TP11	367.3301	367.3319	$C_{22}H_{42}N_2O_2$	12.1			X	X	
TP12	425.3829	425.3850	$C_{24}H_{48}N_4O_2$	12.1			X	X	

Figure 1

Figure 1. (a). First order kinetic constants (k) of UV photolytic treatments for removal of investigated organic pollutants in groundwater employing the flow UV. Three replicates used: Exp 1, Exp 2 and Exp 3. (b). Photolytic degradation of iopromide, terbutaline, BP-1, PFOA and PFOS in groundwater employing the flow UV reactor (light source 40 W Hg lamp, reactor volume: 0.5 L, treated volume: 2 L, recirculation flow rate: 6 L h^{-1}).
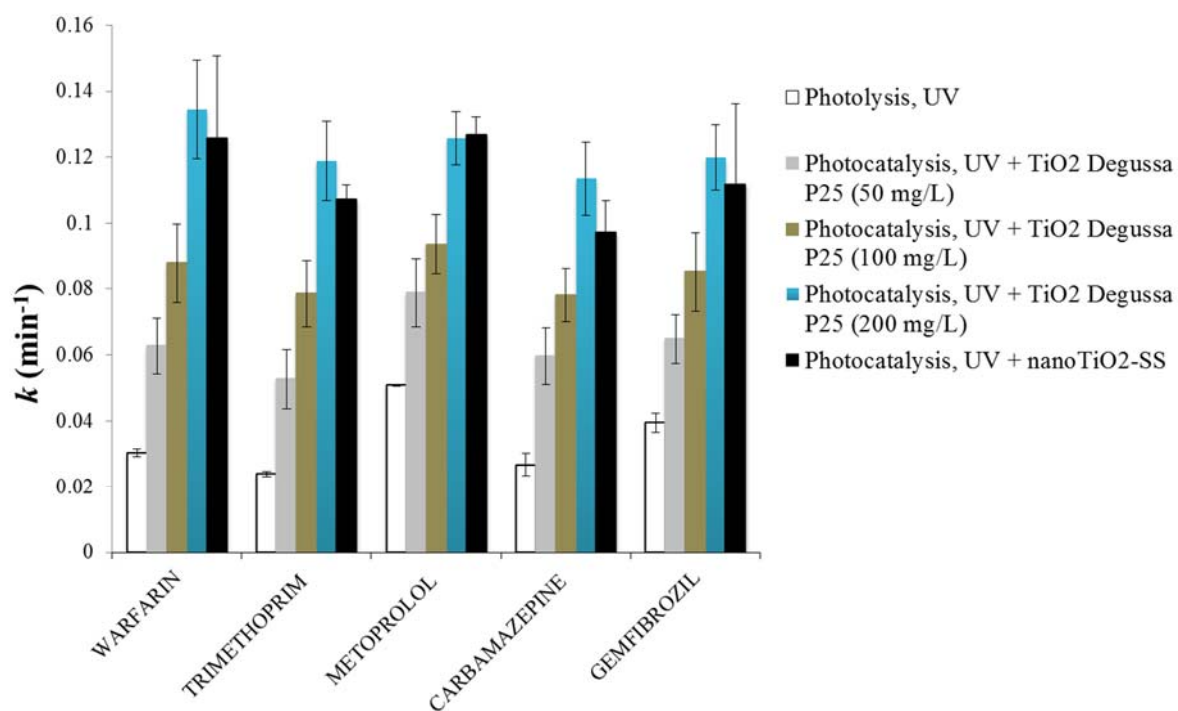
Figure 2

Figure 2. Photocatalytic performance of TiO_2 supported catalyst on stainless steel as compared to photolysis and conventional Degussa P25 for the removal of target emerging pollutants in groundwater (light source 40W Hg lamp, reactor volume: 0.5 L, treated volume: 2 L, recirculation flow rate: 6 L h^{-1}). Error bars = standard deviation of three replicates.